JCTC Journal of Chemical Theory and Computation

Geometries of Transition-Metal Complexes from Density-Functional Theory

Michael Bühl* and Hendrik Kabrede

Max-Planck-Institut für Kohlenforschung, Kaiser-Wilhelm-Platz 1, D-45470 Mülheim an der Ruhr, Germany

Received March 31, 2006

Abstract: Several levels of density functional theory, i.e., various combinations of exchange-correlation functionals and basis sets, have been employed to compute equilibrium geometries for a diverse set of 32 metal complexes from the first transition row, for which precise gas-phase geometries are known from electron diffraction or microwave spectroscopy. Most DFT levels beyond the local density approximation can reproduce the 50 metal−ligand bond distances selected in this set with reasonable accuracy, as assessed by mean and standard deviations of optimized vs observed values. The ranking of some popular functionals, ordered according to decreasing standard deviation, is BLYP ≈ HCTH > B3LYP > BP86 > TPSS ≈ TPSSh. Together with its hybrid variant, the recently introduced meta-GGA functional TPSS performs best of all tested functionals, with mean and standard deviations of −0.5 and 1.4 pm, respectively. Even smaller errors are found for a more compact but less diverse set of transition-metal mono- and dihalides, for which experimentally derived equilibrium geometries are available.

Introduction

Accurate molecular geometries are prerequisite for reliable quantum-chemical computations. The predictive power of high-level ab initio calculations for molecular properties relies on the quality of the geometries for which these properties are evaluated. For molecules composed of lighter main-group atoms, geometrical parameters can usually be calculated reliably at intermediate ab initio levels such as MP2. More sophisticated methods such as CCSD(T) in conjunction with large basis sets afford bond lengths and angles that can even be more accurate than those derived by experiment. The performance of these and other ab initio methods in the calculation of equilibrium bond distances has nicely and instructively been demonstrated by Helgaker and co-workers,[1,2] who assessed each method in terms of mean and standard deviation between optimized and observed bond lengths and visualized these results in the form of normalized Gaussian distributions with the same characteristics. This was done for a set of 19 small molecules (28 distances in total), for which accurate experimental data are available.

* Corresponding author fax: + (0)208-306 2996; e-mail: buehl@mpi-muelheim.mpg.de.

This test set contained only small molecules including main-group atoms up to the first row. It would be highly desirable to be able to achieve a similar accuracy for the more challenging class of transition-metal complexes. These are frequently more demanding than main-group molecules not only in terms of the level of electron correlation that has to be covered but also in terms of size. Thus, CCSD(T) or MR-CI geometry optimizations with sufficiently large basis sets are extremely, usually prohibitively, expensive. For this reason, computational transition-metal chemistry remains a stronghold of methods rooted in modern density functional theory (DFT), as these can account for a large fraction of electron correlation at an affordable cost. The price to be paid is a lower accuracy, compared to that of sophisticated ab initio methods, and the difficulty to improve it systematically. In practice, the density functional best suited for a given problem has to be identified by careful validation against experiment. As far as experimental structures are concerned, this validation is hampered by a dearth of accurate structure determinations in the gas phase, to which the overwhelming majority of DFT applications would refer. Quite frequently, parameters optimized for pristine molecules are compared to those obtained from X-ray crystallography

10.1021/ct6001187 CCC: $33.50
Published on Web 06/30/2006

Chart 1

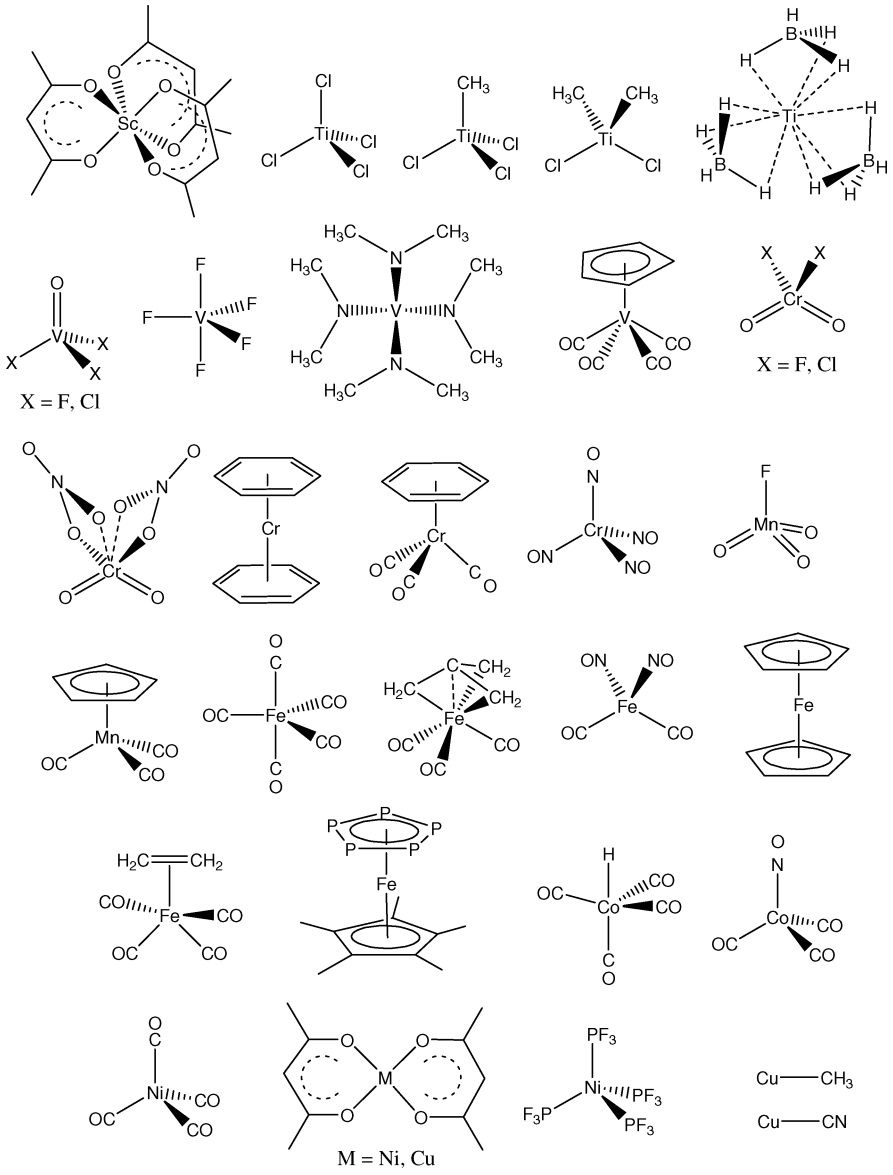

or neutron diffraction, that is, for structures in the solid with unknown effects from packing forces and intermolecular interactions. The overall experience with DFT-optimized geometries is that most gradient-corrected (GGA) or hybrid functionals perform reasonably well, albeit with a tendency to overestimate metal−ligand bond distances by several pm, and with deviations typically increasing from metal−C to metal−P bonds.[3]

Occasionally, newly developed functionals are also tested against gas-phase geometries but usually only for a small number of complexes (see refs 4−8 for a few illustrative examples). We have now selected a much larger test set comprising all 3d metals from Sc to Cu, for which quite precise experimental data are available from gas-phase electron diffraction (GED) and/or microwave spectroscopy (MW). This test set, depicted in Chart 1, should be diverse enough to cover a wide range of bonding situations, from complexes of high-valent early transition metals with electronegative ligands to electron-rich organometallic compounds of middle or late transition metals. Drawing from a large compilation of gas-phase structures,[9] we chose complexes for which at least one metal−ligand bond length was determined with a precision better than 1 pm, affording a final set of 32 molecules with 50 individual bond distances with that precision, which should be sufficient for reasonable statistics. We have then optimized these structures with popular local, gradient-corrected, hybrid, and meta-GGA functionals, together with a variety of basis sets, and assessed each combination, in the spirit of Helgaker and co-workers,[1,2] in terms of mean and standard deviation from the corresponding experimental reference values. As it turns out, the BP86 functional performs best among the traditional GGAs and hybrid functionals, and a recent meta-GGA, TPSS, is slightly superior.

Computational Details

Geometries were fully optimized in the given symmetry (as given in Table 1) using Gaussian 03[10] and several local (LSDA)[11] and gradient-corrected density functional combinations as implemented therein. Most functionals are composed of one of several exchange parts, namely Becke[12] (B), Becke hybrid[13] (B3), OPTX[14] (O), or OPTX hybrid[15] (O3), together

Table 1: Geometrical Parameters (Bond Lengths *r* in pm, Bond Angles *a* in Degrees) of First-Row Transition-Metal Complexes in the Gas Phase[a,b]

compd (mult) *sym*	parameter	[bond no.]	$(r/a)_{a/\alpha}$	$(r/a)_{z/0/av/g}$	ref
$Sc(acac)_3$ (1) D_3	*r*(Sc−O)	[1]	207.6(4)	208.3(4)	36
$TiCl_4$ (1) T_d	*r*(Ti−Cl)	[2]	216.9	217.0(2)	37
$TiMeCl_3$ (1) C_{3v}	*r*(Ti−C)	[3]	204.7(6)		38
	r(Ti−Cl)	[4]	218.5(3)		
	a(Cl−Ti−C)		105.6(2)		
$TiMe_2Cl_2$ (1) C_{2v}	*r*(Ti−C)	[5]	205.8(4)		39
	r(Ti−Cl)	[6]	219.6(3)		
	a(C−Ti−C)		102.8(9)		
	a(Cl−Ti−Cl)		117.3(3)		
$Ti(BD_4)_3$ (2) C_{3h}	*r*(Ti−B)	[7]	217.5(4)		40
	r(Ti-D^{br})	[8]	198.4(5)		
VOF_3 (1) C_{3v}	*r*(V═O)	[9]		157.0(5)	41
	r(V−F)	[10]		172.9(2)	
	a(O−V−F)		107.7(4)		
VF_5 (1) D_{3h}	*r*(V−F^{ax})	[11]	173.4(7)		42
	r(V−F^{eq})	[12]	170.8(5)		
$VOCl_3$ (1) C_{3v}	*r*(V═O)	[13]	157.3(8)	156.8(5)	43
	r(V−Cl)	[14]	213.8(2)	213.8(2)	
	a(Cl−V−Cl)		111.4(4)	111.3(2)	
$V(NMe_2)_4$ (2) S_4	*r*(V−N)	[15]	187.9(4)		44
	a(N−V−N)		100.6(5)		
	a(N−V−N′)		114.1(1)		
$V(Cp)(CO)_4$ (1) C_s	*r*(V−C^{CO})	[16]	196.3(7)		45
CrO_2F_2 (1) C_{2v}	*r*(Cr═O)	[17]	157.4(2)	157.5(2)	46
	r(Cr−F)	[18]	171.9(2)	172.0(2)	
	a(O═Cr═O)		107.8(8)		
	a(F−Cr−F)		111.9(9)		
CrO_2Cl_2 (1) C_{2v}	*r*(Cr═O)	[19]	157.7(2)	158.1(2)	47
	r(Cr−Cl)	[20]	212.2(2)	212.6(2)	
	a(O═Cr═O)		108.5(4)		
	a(Cl−Cr−Cl)		113.3(3)		
$CrO_2(NO_3)_2$ (1) C_2	*r*(Cr═O)	[21]	158.4(2)		48
	r(Cr−O)	[22]	195.4(5)		
$Cr(C_6H_6)_2$ (1) D_{6h}	*r*(Cr−C)	[23]		215.0(2)	49
$Cr(C_6H_6)(CO)_3$ (1) C_{3v}	*r*(Cr−C^{Ar})	[24]	220.8(6)		50
	r(Cr−C^{CO})	[25]	186.3(5)		
	a(C^{CO}-Cr−C^{CO})			87.4(6)[50b]	
$Cr(NO)_4$ (1) T_d	*r*(Cr−N)	[26]	175.0(2)	176.3(2)	51
MnO_3F (1) C_{3v}	*r*(Mn═O)	[27]		158.6(5)	52
	r(Mn−F)	[28]		172.4(5)	
	a(O═Mn−F)			108.5(1)	
$MnCp(CO)_3$ (1) C_1	*r*(Mn−C^{Cp})	[29]	214.7(3)		53
	r(Mn−C^{CO})	[30]	180.6(3)		
$Fe(CO)_5$ (1) D_{3h}	*r*(Fe−C)^{mean}	[31]		182.9(2)	54
	(*r*(Fe−C^{ax})		180.9	181.0(16))	
	(*r*(Fe−C^{eq})		184.1	184.2(11))	
$Fe(CO)_3$(tmm) (1) C_{3v}	*r*(Fe−C^{CO})	[32]		181.0(3)	55
	r(Fe−C^{cent})	[33]		193.8(5)	
	r(Fe−C^{CH2})	[34]		212.3(5)	
	a(Fe−C^{cent}−C^{CH2})			76.4(2)	
$Fe(CO)_2(NO)_2$ (1) C_{2v}	*r*(Fe−C)	[35]	187.2	188.3(3)	51
	r(Fe−N)	[36]	167.4	168.8(3)	
$FeCp_2$ (1) D_{5h}	*r*(Fe−C)	[37]		206.4(3)	56
$Fe(C_2H_4)(CO)_4$ (1) C_{2v}	*r*(Fe−C^{et})	[38]		211.7(4)	57
	r(Fe−C^{ax})	[39]		181.5(2)	
	r(Fe−C^{eq})	[40]		180.6(9)	
	a(C^{eq}-Fe−C^{eq})			111.7(9)	
$Fe(C_5Me_5)(\eta^5\text{-}P_5)$ (1) C_5	*r*(Fe−P)	[41]	237.7(5)		58
$CoH(CO)_4$ (1) C_{3v}	*r*(Co−C^{eq})	[42]	181.8(3)	179.8(2)	59
	a(H−Co−C^{eq})		80.3(6)	81.4(11)	
$Co(CO)_3(NO)$ (1) C_{3v}	*r*(Co−N)	[43]	165.8(6)	167.1(6)	60
	r(Co−C)	[44]	183.0(3)	184.3(3)	
$Ni(CO)_4$ (1) T_d	*r*(Ni−C)	[45]	182.5(2)	183.8(2)	61
$Ni(acac)_2$ (1) D_{2h}	*r*(Ni−O)	[46]		187.6(5)	62
$Ni(PF_3)_4$ (1) T_d	*r*(Ni−P)	[47]	209.9(3)		63
$CuCH_3$ (1) C_{3v}	*r*(Cu−C)	[48]		188.41(2)	64
CuCN(1) $C_{\infty v}$	*r*(Cu−C)	[49]		183.231(7)	65
$Cu(acac)_2$ (2) D_{2h}	*r*(Cu−O)	[50]		191.4(2)	66

[a] Where available, $(r/a)_{a/\alpha}$ values were taken as reference. [b] (In parentheses: multiplicity) acac = acetylacetonato, ax = axial, br = bridging, cent = central, Cp = cyclopentadienyl; eq = equatorial. et = ethylene, tmm = trimethylenemethane [in brackets: running number of bonds].

with one of several correlation parts, namely P86[16] PW91,[17] or LYP[18] (in parentheses: symbols used in combined forms). Other functionals comprise HCTH/407 (denoted HCTH)[6,19] as well as the meta-GGAs BMK,[20] VSXC,[21] TPSS,[22] and TPSS hybrid (denoted TPSSh).[23] A fine integration grid (75 radial shells with 302 angular points per shell) has been used, except for VSXC, which has been shown to require finer grids[24] (here we used 99 radial shells with 590 angular points).

The following basis sets were used: AE1 denotes the Wachters basis (augmented by two diffuse p and one diffuse d sets) on the metals[25] (8s7p4d, full contraction scheme 62111111/3311111/3111) and 6-31G* on the ligands;[26] AE2 stands for the same augmented Wachters basis on the metals, polarized by an additional set of f-functions (exponents 0.60, 0.69, 0.78, 0.87, 0.96, 1.05, 1.17, 1.29, 1.44 for Sc−Cu), and 6-311+G* for the ligands.[27] svp,[28] tzvp,[29] and qzvp[30] are the polarized split-valence basis sets from Ahlrichs and co-workers; the latter qzvp basis has been adopted as in a recent study by Furche and Perdew (i.e. in the 11s6p5d3f1g contraction for the metals).[6] In addition to these all-electron basis sets, small-core effective core potentials (ECPs) with the corresponding valence basis sets were also employed on the metals, namely nonrelativistic LANL2DZ[31] (with [3s3p2d] valence basis and Dunning's double-ζ basis[32] on the ligands), and SDD,[33] i.e., the relativistic Stuttgart-Dresden ECP (together with the [6s5p3d1f] valence basis and 6-31G* basis on the ligands—note that the latter is not supplied with the SDD keyword in the Gaussian program). For essentially all levels, the minimum character of all optimized structures was verified by evaluation of the harmonic vibrational frequencies. Closed- and open-shell species were treated with restricted and unrestricted formalisms, respectively.

Results and Discussion

Selection of Reference Values. In addition to the precision criterion mentioned in the Introduction, we limited our selection to molecules measured at room temperature or slightly above. Thus, the large body of GED data for simple transition-metal di- and trihalides[34] has not been included because typical experimental temperatures reach or exceed 1000 K (see below for selected halides where equilibrium distances have been derived). In many cases, not all degrees of freedom have been refined experimentally, and only mean values for formally nonequivalent distances are known. In those cases, we evaluated and assessed the same average of the corresponding optimized parameters, even though full geometry optimizations were performed. For $Fe(CO)_5$, only the mean value of equatorial and axial Fe−C bond lengths is known with the required precision, and the difference between them is associated with a much larger uncertainty;[54] again, only the mean value was evaluated and assessed.

The final selected experimental parameters are collected in Table 1. Most distances are r_a or r_α values determined from GED (third column in Table 1). When both sets were given in the original papers, r_a values were chosen, as these should be closer to the equilibrium values, r_e. In some cases, only r_z and/or r_0 geometries are known from MW spectroscopy (fourth column in Table 1).[35] When both GED and MW data are available, both sets are given in Table 1, but only the former (third column) has been taken as reference values. In some GED studies, averaged structures (r_{av} or r_g) were derived from force fields and refined amplitudes; when no MW data are known, these values are included in the fourth column of Table 1 for comparison. In most cases, the various data sets are in good mutual accord, with differences on the order of 1 pm. When larger deviations were encountered (e.g. more than 5 pm between r_a and r_g in $Mn(CO)(NO)_3$),[51] these parameters were excluded from the reference set.

Looking at the final set in Chart 1, it seems that high-valent early and low-valent middle and late transition-metal complexes are present in a fairly well-balanced manner. It should be noted, however, that hydride and phosphine complexes are rather under-represented. The only metal−hydrogen distance included in the test set refers to that involving a bridging borane, namely the Ti−D distance in $Ti(BD_4)_3$ (metal−H distances in hydride complexes are ususally associated with large uncertainties, e.g. almost 2 pm for the Co−H bond in $CoH(CO)_4$). In light of the importance of aliphatic and aromatic phosphines as versatile ligands in transition-metal chemistry, the lack of any gas-phase structures of a 3d-metal with these moieties is particularly deplorable. The only metal−P distances included in the test set are those involving PF_3 and cyclic P_5 ligands. It would be highly desirable to have more, accurate reference structures for the important class of phosphine complexes.

Performance of the Models. The distances optimized with selected density-functional/basis-set combinations are given as Supporting Information. The resulting statistical assessment, that is, the mean deviations from the reference data in Table 1, and the standard deviations from those mean values[67] are summarized in Table 2. Deviations are defined as $r_{calc} - r_{exp}$, so that positive mean deviations denote overestimation of the bond lengths by DFT. In addition, the (unsigned) maximum errors are included in Table 1. First, all functionals were tested with the medium-sized basis set denoted AE1, which consists of the augmented all-electron Wachters basis on the metal and 6-31G* basis on the ligands. Second, other basis sets were employed for selected functionals, notably BP86 and B3LYP. Truly large basis sets, such as the generally contracted ANO bases by Roos and co-workers used in benchmark calculations,[68] are quite expensive for routine applications to larger molecules and have therefore not been used. The largest basis employed in this study is the Ahrichs-type qzvp basis from ref 30. The following conclusions can be drawn from our results:

1. LSDA (entry 1) produces much too short bonds, consistent with the well-known tendency for overbinding at that level.[69] This functional should not be used for computations involving 3d-transition metals.

2. Among the "pure" GGAs, BP86 appears to be slightly superior over the other ones, at least in conjunction with the medium-sized AE1 basis (entries 2−5). Most of these GGAs produce quite similar geometries, with the exception of BLYP (entry 3), which tends to overestimate the bond distances considerably (cf. the mean deviation of more than 2 pm).

Table 2: Statistical Assessment of Various Density-Functional/Basis-Set Combinations in Terms of Mean Signed Deviations from the Reference Distances *r* in Table 1,[a] Standard Deviations from These Mean Signed Values, and Absolute Maximum Errors[b,c]

entry	functional	basis set	mean (MAD)	standard	maximum
1	LSDA	AE1	−3.80 (3.82)	2.07	9.46 [35]
2	BP86	AE1	0.35 (1.46)	1.76	4.90 [35]
3	BLYP	AE1	2.31 (2.43)	2.04	6.94 [24]
4	HCTH	AE1	−0.21 (1.71)	2.16	5.50 [50]
5	OLYP	AE1	0.43 (1.71)	2.13	5.97 [50]
6	B3LYP	AE1	0.54 (1.61)	1.87	4.52 [24]
7	O3LYP	AE1	−0.38 (1.64)	1.95	5.31 [35]
8	B3P86	AE1	−1.36 (1.65)	1.57	5.94 [35]
9	BMK	AE1	0.02 (1.89)	2.30	5.42 [41]
10	VSXC	AE1	1.56 (1.83)	1.71	6.20 [24]
11	TPSS	AE1	0.13 (1.12)	1.48	4.44 [35]
12	TPSSh	AE1	−0.51 (1.14)	1.39	4.86 [35]
13	BP86	LANL2DZ	1.05 (3.10)	3.77	12.93 [47]
14	BP86	SDD	−0.63 (1.55)	1.88	5.82 [35]
15	BP86	AE2	0.11 (1.40)	1.75	4.98 [35]
16	BP86	svp	−0.40 (1.58)	1.89	5.73[35]
17	BP86	tzvp	0.43 (1.58)	1.91	5.10 [35]
18	BP86	qzvp	0.02 (1.40)	1.75	5.14 [35]
19	B3LYP	LANL2DZ	1.19 (3.01)	3.98	14.30 [47]
20	B3LYP	SDD	−0.46 (1.73)	2.06	4.41 [35]
21	B3LYP	AE2	0.31 (1.63)	1.99	4.13 [24]
22	B3LYP	svp	−0.21 (1.67)	1.96	4.42 [35]
23	B3LYP	tzvp	0.62 (1.68)	2.00	4.85 [24]
24	B3LYP	qzvp	0.28 (1.61)	1.95	4.14 [24]
25	TPSS	svp	−0.57 (1.32)	1.57	5.16 [35]
26	TPSS	tzvp	0.20 (1.23)	1.57	4.57 [35]
27	TPSS	qzvp	−0.20 (1.17)	1.48	4.70 [35]

[a] In parentheses: mean absolute deviations. [b] In brackets: number of the corresponding bond as identified in Table 1. [c] All values in pm.

3. Inclusion of exact exchange tends to result in decreased bond lengths and slight improvement of the standard deviation with respect to the corresponding nonhybrid functional (compare entries 2 vs 8, 3 vs 6, 5 vs 7, or 11 vs 12). The errors of BLYP are so large, however, that the corrections brought about by the corresponding hybrid functional are not sufficient, and B3LYP is worse than BP86 (with virtually any basis set). B3P86 is superior to BP86 in terms of the standard deviation but produces significantly too short bonds (entry 8).

4. Of the meta-GGAs that have been tested (entries 10 and 11), TPSS affords the best accord with experiment, slightly better even than the best GGA, BP86. The hybrid-variant TPSSh (entry 12) furnishes the lowest standard deviation of all functionals studied here, below 1.4 pm, but is also quite prominent in underestimating the bond lengths. The BMK functional produces a large scatter (cf. the large standard deviation in entry 9), presumably due to the large amount of Hartree−Fock exchange (42%),[20] which, unlike for some reaction barriers, does not appear to be beneficial in our case.

5. The choice of basis set affects mostly the mean deviation from experiment and not the scatter. With BP86, for instance, the standard deviation is virtually the same for the all-electron bases (1.7−1.9 pm, cf. entries 2 and 15−18), whereas the mean error varies between ca. −0.4 and +0.5 pm. These "extreme" values refer to the Ahlrich-type svp and tzvp bases, respectively; the much larger qzvp basis has a mean error between, i.e., close to zero. Similar observations are made with B3LYP (entries 7 and 21−24), with mean deviations increased by ca. 0.2−0.3 pm with respect to the corresponding BP86 values.

6. The relativistic Stuttgart-Dresden pseudopotential (included in SDD, entries 14 and 20) affords shorter bonds and a somewhat larger scatter than obtained with similar all-electron basis sets (compare e.g. entries 7 and 20). The Hay-Wadt pseudopotential was tested only in conjunction with a very small DZ basis on the ligands, a popular combination for routine applications in the literature. Clearly, this basis is much too small, and the resulting LANL2DZ level has the lowest precision of all, judged by the large standard deviation of almost 4 pm (entries 13 and 19). The shortcoming of this small basis is particularly pronounced for distances to the second-row element P, which are overestimated by more than 10 pm (cf. maximum errors for entries 13 and 19 in Table 2).

Compared to the distances, less attention was paid to the bond angles. In the whole test set, there are only 15 angles about the metal centers that are not dictated by symmetry and that have been refined with a precision better than 1°. These angles *a* cover the range between ca. 77° and 117° and are included in Table 1. At most levels studied, these angles are reproduced within ±0.1° (mean error) and a standard deviation around ca. 1.2°−1.5°, with little discrimination between the various functional/basis combinations.

To conclude this section, most GGAs are quite robust in reproducing geometries of transition-metal complexes, and effects of exact exchange or basis sets are usually small or moderate. The TPSS meta-GGA as well as its hybrid variant furnishes the most accurate metal−ligand distances, as judged from the reasonably small standard deviation from experiment, ca. 1.4 pm. The best GGA is BP86, slightly superior to B3LYP. The performance of these three functionals is shown schematically in Figure 1a, a plot of normalized Gaussian distributions using the corresponding data from Table 1 (analogous to the presentation by Helgaker et al.).[1,2] Figure 1b illustrates the basis-set dependence for one particular density functional, BP86, where increase of the basis results in but small shifts of the normal distribution, and hardly affects its width.

When assessing the results in terms of mean deviations from experiment, it should be kept in mind that calculated equilibrium geometries are compared to mean or effective observed ones. Thus, perfect agreement (i.e. zero mean deviation) is not to be expected, and the optimized distances should be systematically shorter than the experimental ones. In principle, equilibrium distances can be deduced from GED experiments, provided accurate force fields and refined vibrational amplitudes are available (see section on dihalides below).[70] Such analyses are rather involved, however, and

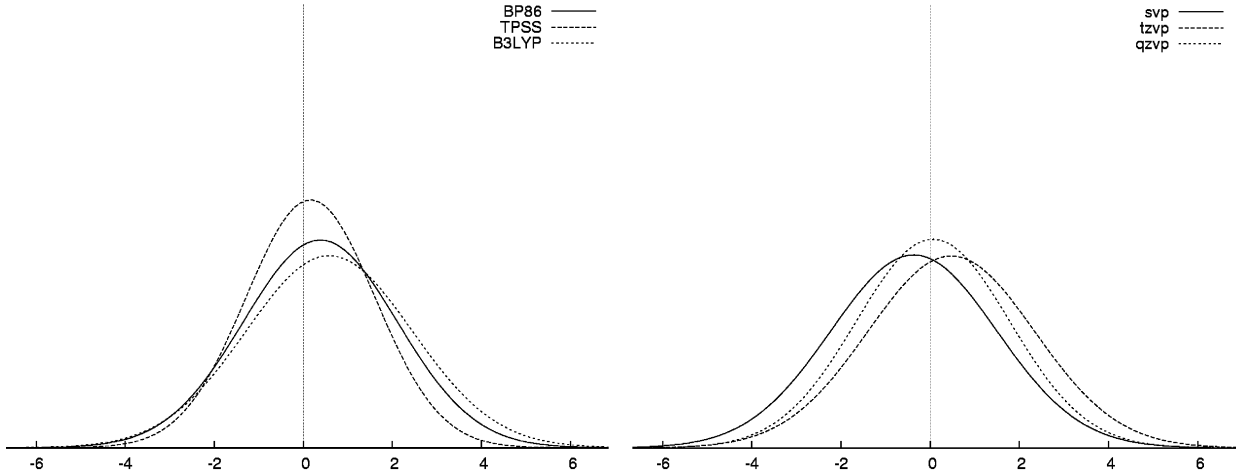

Figure 1. Normal distributions for the errors in the optimized bond distances for the test set in Chart 1. The distributions have been calculated from the mean and standard deviations in Table 2 and are all normalized to one: (a) left, dependence on the density functional using AE1 basis and (b) right, dependence on the basis set for the BP86 functional.

therefore rare. A recent example comprises ferrocene, for which an equilibrium r_e(Fe−C) distance of 205.4(3) pm has been inferred,[71] 1 pm shorter than the r_a value in Table 1. Rovibrational corrections to equilibrium bond distances can also be computed quantum-mechanically (from anharmonic force fields).[72] We have recently computed zero-point effects, which contribute significantly to these corrections, for a number of Ti-, V-, Mn-, Fe-, and Co-complexes.[73] In the vast majority of cases, such zero-point corrections tend to increase bond distances from their r_e values, by up to ca. 1 pm.[74] This value, which is comparable to the precision of the chosen experimental parameters, thus marks a lower limit for the degree of agreement that one can hope to achieve in our analysis.

In addition, GED results for transition-metal complexes, even when reasonably precise, need not necessarily be highly accurate. If any decomposition reactions during vaporization of the samples go undetected, the observed radial distributions and, thus, the structural parameters derived thereof may be affected noticeably. In view of these limitations, the performance of most DFT methods is actually quite satisfactory. However, an accuracy as that achievable with highly sophisticated ab initio methods for equilibrium bond distances of light main-group compounds (eg. mean and standard deviation around 0.2 and 0.3 pm, respectively, at CCSD(T)/cc-pVQZ)[1,75] appears to be out of reach, or at least undetectable, for transition-metal complexes.

Performance for Simple Halides. As mentioned above, experimental structures determined at very high temperatures T were not included in the test set, because the shift of thermally averaged parameters from their equilibrium values is expected to increase with T. For a number of transition-metal dihalides MX_2 (M = Mn, Fe, Co, Ni, X = F, Cl), however, facilitated by their high symmetry, such high-temperature GED studies in combination with vibrational spectroscopy have been used to deduce equilibrium bond distances. These r_e values (collected in Table 3), which can be directly compared with the DFT optimizations, are different in nature from the effective or averaged parameters in Table 1. Hence, we decided to evaluate the results for these dihalides, together with those from the diatomics CuF and CuCl (for which accurate equlibrium geometries are also known), separately. Mean and standard deviations for DFT geometries[76] are collected in Table 4.

Table 3: Experimental Equilibrium Bond Lengths (r_e in pm) of First-Row Transition-Metal Halides in the Gas Phase[a]

compd (mult)	[bond no.]	r_e(M−X)	ref
MnF_2 (6)	[51]	179.7(6)	79
FeF_2 (5)	[52]	175.5(6)	79
CoF_2 (4)	[53]	173.8(6)	79
NiF_2 (3)	[54]	171.5(7)	79
CuF (1)	[55]	174.4922(21)	80
$MnCl_2$ (6)	[56]	218.4(5)	81
$FeCl_2$ (5)	[57]	212.8(5)	81
$CoCl_2$ (4)	[58]	209.0(5)	81
$NiCl_2$ (3)	[59]	205.6(5)	81
CuCl (1)	[60]	205.11778(8)	82

[a] In parentheses: multiplicity; in brackets: running number of bonds.

Evidently, with just 10 distances this subset is smaller and less diverse than the larger test set of Chart 1. However, very similar conclusions can be drawn regarding the performance of the various exchange-correlation functionals. For instance, BP86 (together with the related BPW91) performs best among the GGAs, clearly better than B3LYP, and slightly inferior only to TPSS (see Figure 2 for a graphical representation).[77] Basis-set effects tend to be similar for the halides and the larger test set as far as the mean error is concerned, but for the halides the standard deviation is somewhat more sensitive to basis-set enlargement, which affords a noticeable improvement (compare e.g. the svp-tvzp-qzvp triads in Table 4, such as entries 30−32). LANL2DZ is very poor throughout, in keeping with similar findings in the literature.[78]

Again, TPSS and its hybrid variant produce the best results, with mean and standard deviations around ca. ±0.2 and 0.8 pm, respectively. These functionals thus emerge as very promising tools for first-principles calculations of transition-metal complexes. Other recent studies, which also

Table 4: Statistical Assessment of the Various Density-Functional/Basis-Set Combinations in Terms of Mean, Signed Deviations from the Reference Distances in Table 3,[a] Standard Deviations from These Mean Signed Values, and Absolute Maximum[b,c]

entry	functional	basis set	mean (MAD)	standard	maximum
1	LSDA	AE1	−4.37 (4.36)	0.74	5.29 [57]
2	BP86	AE1	−0.21 (0.88)	1.09	2.17 [60]
3	BLYP	AE1	1.17 (1.33)	1.47	4.16 [60]
4	HCTH	AE1	0.63 (0.88)	1.16	3.43 [60]
5	OLYP	AE1	1.15 (1.35)	1.37	4.05 [60]
6	BPW91	AE1	0.07 (0.79)	1.09	2.49 [60]
7	B3LYP	AE1	1.07 (1.49)	1.66	4.20 [60]
8	O3LYP	AE1	1.03 (1.34)	1.50	4.15 [60]
9	B3P86	AE1	−0.21 (0.95)	1.23	2.40 [60]
10	B3PW91	AE1	0.36 (1.05)	1.31	3.03 [60]
11	BMK	AE1	1.75 (2.04)	1.99	5.07 [60]
12	VSXC	AE1	1.42 (1.53)	1.43	4.20 [60]
13	TPSS	AE1	−0.02 (0.87)	1.09	2.17 [60]
14	TPSSh	AE1	0.19 (0.98)	1.21	2.55 [60]
15	BP86	LANL2DZ	4.08 (4.08)	2.53	8.91 [60]
16	BP86	SDD	−0.32 (1.33)	1.25	1.78 [51]
17	BP86	AE2	0.54 (0.89)	1.24	2.80 [59]
18	BP86	svp	−0.06 (0.99)	1.23	2.17 [60]
19	BP86	tzvp	0.87 (0.96)	1.14	3.22 [60]
20	BP86	qzvp	−0.46 (0.93)	0.98	1.69 [55]
21	B3LYP	LANL2DZ	6.44 (6.44)	2.73	10.11 [60]
22	B3LYP	SDD	1.82 (2.62)	2.65	5.39 [59]
23	B3LYP	AE2	2.04 (2.04)	1.33	4.83 [60]
24	B3LYP	svp	1.08 (1.54)	1.70	4.01 [60]
25	B3LYP	tzvp	2.27 (2.27)	1.54	5.54 [60]
26	B3LYP	qzvp	1.24 (1.24)	1.14	3.59 [60]
27	TPSS	LANL2DZ	4.69 (4.69)	2.64	9.50 [60]
28	TPSS	SDD	0.74 (2.08)	1.71	3.86 [54]
29	TPSS	AE2	0.70 (0.82)	1.02	2.58 [60]
30	TPSS	svp	0.24 (1.12)	1.36	2.42 [60]
31	TPSS	tzvp	1.00 (1.00)	1.03	3.18 [60]
32	TPSS	qzvp	−0.16 (0.60)	0.73	1.17 [55]
33	TPSSh	LANL2DZ	4.71 (4.71)	2.63	9.63 [60]
34	TPSSh	SDD	0.87 (1.67)	1.72	3.51 [54]
35	TPSSh	AE2	0.88 (0.91)	1.05	2.92 [60]
36	TPSSh	svp	0.47 (1.20)	1.46	2.76 [60]
37	TPSSh	tzvp	1.18 (1.18)	1.12	3.57 [60]
38	TPSSh	qzvp	0.06 (0.58)	0.77	1.46 [60]

[a] In parentheses: mean absolute deviations. [b] In brackets: number of the corresponding bond as identified in Table 3. [c] All values in pm.

included assessments of computed binding and reaction energies,[6,83] reached the same conclusion.

Conclusions

We have tested a number of density-functional/basis-set combinations for their ability to reproduce experimental bond distances of transition-metal complexes in the gas phase. For this purpose, two test sets were selected from the literature, a larger one containing 50 effective or averaged metal−ligand distances, and a smaller one with 10 equilibrium metal−halide bond lengths. Care has been taken to include only parameters that have been determined with sufficient precision (all better than 1 pm, most better than 0.5 pm). Among the traditional GGAs, BP86 performs best, better than the popular B3LYP combination. In general, hybrid functionals furnish only minor improvements over their nonhybrid variants. The best results are obtained with a recently introduced meta-GGA, TPSS, with or without exact exchange included. Our findings thus corroborate other recent studies that had attested great potential of this functional for computational transition-metal chemistry. We have now established a solid ground for the assessment of molecular geometries in this area, upon which not only performance tests of other contemporary or future exchange-correlation functionals but also high-level ab initio methods can be based.

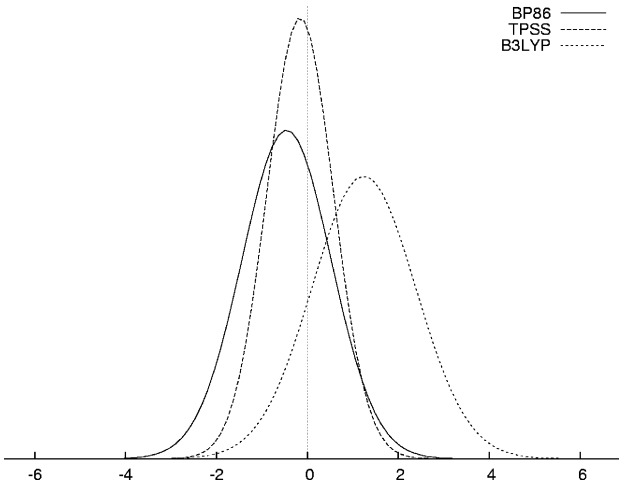

Figure 2. Normal distributions for the errors in the equilibrium bond distances in mono- and dihalides. The distributions have been calculated from the mean and standard deviations in Table 4, normalized to one, and drawn to scale with the plots in Figure 1. Selected density functionals have been employed, together with qzvp basis.

Acknowledgment. M.B. wishes to thank Prof. W. Thiel, the MPI Mülheim, and the Deutsche Forschungsgemeinschaft for continuing support. We thank H. Lenk for technical assistance. Computations were performed on an Intel Xeon and Opteron PC cluster at the MPI Mülheim.

Supporting Information Available: Bond distances of the test set in Table 1, optimized at selected levels, and BP86/qzvp optimized Cartesian coordinates. This material is available free of charge via the Internet at http://pubs.acs.org.

References

(1) Helgaker, T.; Gauss, J.; Jørgensen, P.; Olsen, J. *J. Chem. Phys.* **1997**, *106*, 6430−6440.

(2) Bak, K. L.; Gauss, J.; Jørgensen, P.; Olsen, J.; Helgaker, T.; Stanton, J. F. *J. Chem. Phys.* **2001**, *114*, 6548−6556.

(3) See for instance: Bray, M. R.; Deeth, R. J.; Paget, V. J.; Sheen, P. D. *Int. J. Quantum Chem.* **1997**, *61*, 85−91.

(4) Rosa, A.; Ehlers, A. W.; Baerends, E. J.; Snijders, J. C.; te Velde, G. *J. Phys. Chem.* **1996**, *100*, 5690−5696.

(5) Filatov, M.; Thiel, W. *Phys. Rev. A* **1998**, *57*, 189−199.

(6) Hamprecht, F. A.; Cohen, A. J.; Tozer, D. J.; Handy, N. C. *J. Chem. Phys.* **1998**, *109*, 6264−6271.

(7) (a) Schultz, N. E.; Zhao, Y.; Truhlar, D. G. *J. Phys. Chem. A* **2005**, *109*, 4388−4403. (b) Schultz, N. E.; Zhao, Y.; Truhlar, D. G. *J. Phys. Chem. A* **2005**, *109*, 11127−11143.

(8) Furche, F.; Perdew, J. P. *J. Chem. Phys*. **2006**, *124*, 044103.

(9) *Landolt-Börnstein, Structure Data of Free Polyatomic Molecules*; Kuchitsu, K., Ed.; Springer-Verlag: Berlin, 1998; New Series, Vol. II/25.

(10) M. J. Frisch, G. W. Trucks, H. B. Schlegel, G. E. Scuseria, M. A. Robb, J. R. Cheeseman, J. A. Montgomery, Jr., T. Vreven, K. N. Kudin, J. C. Burant, J. M. Millam, S. S. Iyengar, J. Tomasi, V. Barone, B. Mennucci, M. Cossi, G. Scalmani, N. Rega, G. A. Petersson, H. Nakatsuji, M. Hada, M. Ehara, K. Toyota, R. Fukuda, J. Hasegawa, M. Ishida, T. Nakajima, Y. Honda, O. Kitao, H. Nakai, M. Klene, X. Li, J. E. Knox, H. P. Hratchian, J. B. Cross, C. Adamo, J. Jaramillo, R. Gomperts, R. E. Stratmann, O. Yazyev, A. J. Austin, R. Cammi, C. Pomelli, J. W. Ochterski, P. Y. Ayala, K. Morokuma, G. A. Voth, P. Salvador, J. J. Dannenberg, V. G. Zakrzewski, S. Dapprich, A. D. Daniels, M. C. Strain, O. Farkas, D. K. Malick, A. D. Rabuck, K. Raghavachari, J. B. Foresman, J. V. Ortiz, Q. Cui, A. G. Baboul, S. Clifford, J. Cioslowski, B. B. Stefanov, G. Liu, A. Liashenko, P. Piskorz, I. Komaromi, R. L. Martin, D. J. Fox, T. Keith, M. A. Al-Laham, C. Y. Peng, A. Nanayakkara, M. Challacombe, P. M. W. Gill, B. Johnson, W. Chen, M. W. Wong, C. Gonzalez, J. A. Pople, *Gaussian 03*; Gaussian, Inc.: Pittsburgh, PA, 2003.

(11) Vosko, S. H.; Wilk, L.; Nusair, M. *Can. J. Phys*. **1980**, *58*, 1200−1211; functional III of that paper has been used.

(12) Becke, A. D. *Phys. Rev. A* **1988**, *38*, 3098−3100.

(13) Becke, A. D. *J. Chem. Phys.* **1993**, *98*, 5648−5642.

(14) Handy, N. C.; Cohen, A. J. *Mol. Phys*. **2001**, *99*, 403−412.

(15) Cohen, A. J.; Handy, N. C. *Mol. Phys*. **2001**, *99*, 607−615.

(16) (a) Perdew, J. P. *Phys. Rev. B* **1986**, *33*, 8822−8824. (b) Perdew, J. P. *Phys. Rev. B* **1986**,*34*, 7406.

(17) (a) Perdew, J. P. In *Electronic Structure of Solids*; Ziesche, P., Eischrig, H., Eds.: Akademie Verlag: Berlin, 1991. (b) Perdew, J. P.; Wang, Y. *Phys. Rev. B* **1992**, *45*, 13244−13249.

(18) Lee, C.; Yang, W.; Parr, R. G. *Phys. Rev. B* **1988**, *37*, 785−789.

(19) Boese, A. D.; Handy, N. C. *J. Chem. Phys*. **2001**, *114*, 5497−5503.

(20) Boese, A. D.; Martin, J. M. L. *J. Chem. Phys.* **2004**, *121*, 3405−3416.

(21) Van Voorhis, T.; Scuseria, G. E. *J. Chem. Phys.* **1998**, *109*, 400−410.

(22) (a) Tao, J.; Perdew, J. P.; Staroverov, V. N.; Scuseria, G. E. *Phys. Rev. Lett*. **2003**, *91*, 146401. (b) Perdew, J. P.; Tao, J.; Staroverov, V. N.; Scuseria, G. E. *J. Chem. Phys*. **2004**, *120*, 6898−6911.

(23) (a) Staroverov, V. N.; Scuseria, G. E.; Tao, J.; Perdew, J. P. *J. Chem. Phys*. **2003**, *119*, 12129-12137. (b) Staroverov, V. N.; Scuseria, G. E.; Tao, J.; Perdew, J. P. *J. Chem. Phys*. **2004**, *121*, 11507.

(24) Johnson, E. R.; Wolkow, R. A.; DiLabio, G. A. *Chem. Phys. Lett*. **2004**, *394*, 334−338.

(25) (a) Wachters, A. J. H. *J. Chem. Phys.* **1970**, *52*, 1033−1036. (b) Hay, P. J. *J. Chem. Phys.* **1977**, *66*, 4377−4384.

(26) (a) Hehre, W. J.; Ditchfield, R.; Pople, J. A. *J. Chem. Phys.* **1972**, *56*, 2257−2261. (b) Hariharan, P. C.; Pople, J. A. *Theor. Chim. Acta* **1973**, *28*, 213−222.

(27) (a) Krishnan, R.; Binkley, J. S.; Seeger, R.; Pople, J. A. *J. Chem. Phys*. **1980**, *72*, 650−654. (b) Clark, T.; Chandrasekhar, J.; Spitznagel, G. W.; Schleyer, P. v. R. *J. Comput. Chem.* **1983**, *4*, 294−301.

(28) Schäfer, A.; Horn, H.; Ahlrichs, R. *J. Chem. Phys*. **1992**, *97*, 2571−2577.

(29) Schäfer, A.; Huber, C.; Ahlrichs, R. *J. Chem. Phys*. **1994**, *100*, 5829−5835.

(30) Weigend, F.; Furche, F.; Ahlrichs, R. *J. Chem. Phys*. **2003**, *119*, 12753−12762.

(31) Hay, P. J.; Wadt, W. R. *J. Chem. Phys.* **1985**, *82*, 299−310.

(32) Dunning, T. H.; Hay, P. J. In *Modern Theoretical Chemistry;* Schaefer, H. F., Ed.; Plenum Press: New York, 1977; Vol. 4, pp 1−27.

(33) Dolg, M.; Wedig, U.; Stoll, H.; Preuss H. *J. Chem. Phys.* **1987**, *86*, 866.

(34) Review: Hargittai, M. *Chem. Rev*. **2000**, *100*, 2233−2301.

(35) r_e is the equilibrium distance between the positions of the nuclei on the potential energy surface, r_a is the effective internuclear distance as derived from electron scattering intensities, r_α is the distance between average nuclear positions in the thermal equilibrium at temperature T, r_z is the distance between average nuclear positions in the ground vibrational state, r_0 is the effective internuclear distance obtained from the rotational constants, r_{av} and r_g are the average internuclear distance at temperature T; see e.g.: Hargittai, I. In *Stereochemical Applications of Gas-Phase Electron Diffraction, Part A: The Electron Diffraction Technique*; Hargittai, I., Hargittai, M., Eds.; VCH Publisher: Weinheim, 1988; pp 1−54.

(36) Belova, N. V.; Giricheva, N. I.; Girichev, G. V.; Shlykov, S. A.; Tverdova, N. V.; Kuz'mina, N. P.; Zaitseva, I. G. *J. Struct. Chem*. **2002**, *43*, 56−63.

(37) Morino, Y.; Uehara, H. *J. Chem. Phys*. **1966**, *45*, 4543−4550.

(38) Briant, P.; Green, J.; Haaland, A.; Møllendal, M.; Rypdal, K.; Tremmel, J. *J. Am. Chem. Soc.* **1989**, *111*, 3434−3436.

(39) McGrady, G. S.; Downs, A. J.; McKean, D. C.; Haaland, A.; Scherer, W.; Verne, H.-P.; Holden, H. V. *Inorg. Chem*. **1996**, *35*, 4713−4718.

(40) Dain, C. J.; Downs, A. J.; Goode, M. J.; Evans, D. G.; Nicholls, K. T.; Rankin, D. W. H.; Robertson, H. E. *J. Chem. Soc., Dalton Trans*. **1991**, 967−977.

(41) Almenningen, A.; Samdal, S. *J. Mol. Struct*. **1978**, *48*, 69−78.

(42) Hagen, K.; Gilbert, M. M.; Hedberg, L.; Hedberg, K. *Inorg. Chem*. **1982**, *21*, 2690−2693.

(43) (a) Karakida, K.-I.; Kuchitsu, K. *Inorg. Chim. Acta* **1975**, *13*, 113−119. Very similar GED data in (b) Oberhammer, H.; Strähle, J. *Z. Naturforsch*. **1975**, *30a*, 296−303.

(44) Haaland, A.; Rypdal, K.; Volden, H. V.; Andersen, R. A. *J. Chem. Soc., Dalton Trans*. **1992**, 891−895.

(45) Almond, M. J.; Page, E. M.; Rice, D. A.; Hagen, K. *J. Organomet. Chem*. **1996**, *511*, 303−307.

(46) French, C. R. J.; Hedberg, L.; Hedberg, K.; Gard, G. L.; Johnson, B. M. *Inorg. Chem*. **1983**, *22*, 892−895.

(47) Marsden, C. J.; Hedberg, L.; Hedberg, K. *Inorg. Chem*. **1982**, *21*, 1115−1118.

(48) Marsden, C. J.; Hedberg, K.; Ludwig, M. M.; Gard, G. L. *Inorg. Chem*. **1991**, *30*, 4761−4766.

(49) Haaland, A. *Acta Chem. Scand*. **1965**, *19*, 41−46.

(50) Assuming equal CC bond lengths: (a) Chiu, N.-S.; Schäfer, L. *J. Organomet. Chem*. **1975**, *101*, 331−346. Similar CrC distances (with somewhat larger uncertainties) have been inferred from microwave studies: (b) Sickafoose, S. M.; Breckenridge, S. M.; Kukolich, S. G. *Inorg. Chem*. **1994**, *33*, 5176−5179. For evidence for alternating CC bonds see e.g. (c) Kukolich, S. G. *J. Am. Chem. Soc*. **1995**, *117*, 5512−5514.

(51) Hedberg, L.; Hedberg, K.; Satija, S. K.; Swanson, B. I. *Inorg. Chem*. **1985**, *24*, 2766−2771: r_α values calculated from mean $<M_C,M_N>$ and difference $\Delta(M_C,M_N)$ distances.

(52) (a) Javan, A.; Engelbrecht, A. *Phys. Rev*. **1954**, *96*, 649−658. For a complete recent assignment of the microwave spectrum, see: (b) Bürger, H.; Weinrath, P.; Dressler, S.; Hansen, T.; Thiel, W. *J. Mol. Spectrosc*. **1997**, *183*, 139−150.

(53) Almond, M. J.; Page, E. M.; Rice, D. A.; Hagen, K.; Volden, H. V. *J. Mol. Struct*. **1994**, *319*, 223−230; $Mn-C^{Cp}$ calculated from $r_\alpha(Mn-X) = 1.773(3)$ Å and $r_a(CC) = 1.423(2)$ Å from ree rotation model.

(54) McClelland, B. W.; Robiette, A. G.; Hedberg, L.; Hedberg, K. *Inorg. Chem*. **2001**, *40*, 1358−1362.

(55) Almenningen, A.; Haaland, A.; Wahl, K. *Acta Chem. Scand.* **1969**, *23*, 1145−1150.

(56) Haaland, A.; Nilsson, J. E. *Acta Chem. Scand*. **1968**, *22*, 2653−2670.

(57) Droiun, B. J.; Kukolich, S. G. *J. Am. Chem. Soc*. **1999**, *121*, 4023−4030.

(58) Blom, R.; Brück, T.; Scherer, O. J. *Acta Chem. Scand*. **1989**, *43*, 458−462.

(59) (a) MW: Kukoloch, S. G.; Sickafoose, S. M. *J. Chem. Phys*. **1996**, *105*, 3466−3471. (b) GED: McNeill, E. A.; Scholer, F. R. *J. Am. Chem. Soc*. **1977**, *99*, 6243−6249. In this case, the MW parameters were taken as reference, because the relative sequence of $r(Co-C^{ax})$ and $r(Co-C^{eq})$ appears suspect in the GED structure; $r(Co-H)$ and $r(Co-C^{ax})$ have not been used because of large uncertainties in both studies.

(60) Hedberg, K.; Hedberg, L.; Hagen, K.; Ryan, R. R.; Jones, L. H. *Inorg. Chem*. **1985**, *24*, 2771−2774.

(61) Hedberg, L.; Iijima, T.; Hedberg, K. *J. Chem. Phys*. **1979**, *70*, 3224−3229.

(62) Shibata, S.; Ohta, M.; Tani, R. *J. Mol. Struct*. **1981**, *73*, 119−124.

(63) (a) Almenningen, A.; Andersen, B.; Astrup, E. E. *Acta Chem. Scand*. **1970**, *24*, 1579−1584. A similar distance with a larger uncertainty has been determined independently: (b) Marriott, J. C.; Salthouse, J. A.; Ware, M. J. *J. Chem. Soc., Chem. Commun*. **1970**, 595−596.

(64) MW, r_0 value: Grotjahn, D. B.; Halfen, D. T.; Ziurys, L. M.; Cooksy, A. L. *J. Am. Chem. Soc.* **2004**, *126*, 12621−12627.

(65) MW, r_0 value: Grotjahn, D. B.; Brewster, M. A.; Ziurys, L. M. *J. Am. Chem. Soc*. **2002**, *124*, 5895−5901.

(66) Shibata, S.; Sasase, T.; Ohta, M. *J. Mol. Struct*. **1983**, *96*, 347−352.

(67) Defined, e.g., in eqs 2 and 3 in ref 1.

(68) Pouamerigo, R.; Merchan, M.; Nebotgil, I.; Widmark, P. O.; Roos, B. O. *Theor. Chim. Acta* **1995**, *92*, 149−181.

(69) See for instance: Koch, W.; Holthausen, M. C. *A Chemist's Guide to Density Functional Theory*, 2nd ed.; Wiley-VCH: Weinheim, 2001.

(70) See e.g.: *Stereochemical Applications of Gas-Phase Electron Diffraction, Part A: The Electron Diffraction Technique*; Hargittai, I., Hargittai, M., Eds.; VCH: Weinheim, 1988.

(71) Coriani, S.; Haaland, A.; Helgaker, T.; Jørgensen, P. *ChemPhysChem* **2006**, *7*, 245−249.

(72) See e.g.: Solomonik, V. G.; Stanton, J. F.; Boggs, J. E. *J. Chem. Phys*. **2005**, *122*, 094322.

(73) (a) Bühl, M.; Mauschick, F. T. *Magn. Reson. Chem*. **2004**, *42*, 737−744. (b) Grigoleit, S.; Bühl, M. *Chem. Eur. J*. **2004**, *10*, 5541−5552. (c) Grigoleit, S.; Bühl, M. *J. Chem. Theory Comput.* **2005**, *1*, 181−193.

(74) Computed at BP86/AE1; specific values for the compounds of this study are collected in Table S2 of the Supporting Information (9 complexes with 15 bonds in total). Here, the computed zero-point corrections to bond distances range from 0 to +0.4 pm for metal−ligand single bonds and from +0.6 to +0.7 pm for metal−carbon distances involving π-bonded ligands. Unfortunately, computation of these corrections for all molecules of the test set would be a formidable task beyond the scope of the present paper.

(75) Further, minor improvements for the correlated ab initio methods are brought about by basis sets augmented with diffuse and core-polarization functions, cf. ref 2. For the same set as employed in ref 1, we obtain mean and standard deviations of 0.7 and 0.6 pm, respectively, at TPSS/cc-pVQZ.

(76) At BP86/AE1, only linear minima could be located for all dihalides; thus all subsequent computations were done in $D_{\infty h}$ symmetry.

(77) For other classes of compounds, somewhat different performances of DFT methods may occur: e.g., for r_e values in coordinatively unsaturated diatomics involving first-row transition-metal atoms (including multiply bonded metal dimers), LSDA performs better than GGA or meta-GGA, and the quality of the results deteriorates upon inclusion of Hartree−Fock exchange, cf ref 7.

(78) Strassner, T.; Taige, M. A. *J. Chem. Theor. Comput*. **2005**, *1*, 848−855.

(79) Vogt, N. *J. Mol. Struct*. **2001**, *570*, 189−195.

(80) Hoeft, J.; Lovas, F. J.; Tiemann, E.; Törring, T. *Z. Naturforsch*. **1970**, *25a*, 35−39.

(81) Hargittai, M.; Subbotina, N. Y.; Kolonits, M.; Gershikov, A. G. *J. Chem. Phys*. **1991**, *94*, 7278−7286.

(82) Manson, E. L.; De Lucia, F. C.; Gordy, W. *J. Chem. Phys.* **1975**, *62*, 1040−1043.

(83) Quintal, M. M.; Karton, A.; Iron, M. A.; Boese, D.; Martin, J. M. L. *J. Phys. Chem. A* **2006**, *110*, 709−716.

CT6001187